

PROPERTIES OF POLYPHASE SIGNALS BASED ON THE GENERALIZED FRANK CODES

Roman Yankevych, Ivan Prudyus, Markiyan Sumyk

Lviv Polytechnic National University
roman.yankevych@gmail.com

Abstract. In this paper the results of different kinds of complex polyphase signals based on Frank codes are given.

Keywords. Complex signals, signal processing, specter, autocorrelation, ambiguity function.

1. Introduction

Effectiveness of the objects and scenes monitoring systems is, to a great extent, defined by the accuracy of the angle and distance coordinates measurements. Such measurements can be realized under any weather conditions, at day or night only by using the radar systems [1]. The characteristics mentioned above, hindrance immunity and reliability of the radar systems greatly depend on a type of the probe signal.

In the radar systems only known signals are formed and radiated, so the parameters of the signals change in the process of their spreading in the space or when they are reflected from different objects [2]. The information, obtaining of which is the task of the radar system, contains in these changed, unknown in advance, parameters of the signals. To determine the properties of such signals, possibilities of their application in the construction of different radio-technical systems it is not enough to know their time and frequency characteristics, but it is also important to know the correlation characteristics of these signals, including the ambiguity functions.

Well known and already applied signals can't meet the growing demands to monitoring systems. So the search for new algorithms of forming of the new classes of the complex polyphase signals is conducted. One of those signals classes are the signals based on the generalized Frank codes [3].

The properties of the signals mentioned above are not enough researched. In the paper the results of the properties investigations of several different types of the mentioned signals are shown.

2. Theoretical Part

As generalized Frank code (GFC) we define a discrete complex signal which consists of the sequence of elementary signals, amplitude and phase which we get according to the algorithm [4]:

$$\theta_s = \theta_{nm} = nm \frac{2\pi}{N}, 0 \leq n \leq N-1, 0 \leq m \leq M-1;$$

$$A_s = \begin{pmatrix} 1, 0 \leq m \leq L-1 \\ 0, L \leq m \leq M-1 \end{pmatrix} \quad (1)$$

where N – signal phase levels value.

Generalized Frank code is formed as follows. A time domain equal to the duration of the signal T_s is divided in $S=MN$ temporal positions of duration $\tau_0=T_s/S$. On each of these temporal positions radio signals with frequency ω_0 are formed, rounding and initial phase which is chosen according to the algorithm (1).

The algorithm of GFC forming becomes clearer when the following complex matrix, shown in figure1, is used.

A radio frequency signal is created by the row-to-row writing down of the matrix and transferring of the sequence on the carrier frequency ω .

With the use of the M -metric system of calculus, the ambiguity function equation [3] in the discrete points $\frac{k}{\Delta f}$ (k – integer, $1/\Delta f$ – discretization interval after Kotelnikov) will be the following.

For $M=L$

$$\chi(\tau, f) = \sqrt{A_1^2 + B_1^2 + 2A_1B_1 \cos \left((NL - 2L + 1) \frac{\pi}{N} \right)} \quad (2)$$

where

$$A_1 = \frac{\sin \left((L - g) \left(\frac{r\pi}{N} - \frac{\pi f}{\Delta f} \right) \right)}{\sin \left((L - g) \frac{\pi}{N} - \frac{L\pi f}{\Delta f} \right)} \times \frac{\sin \left((N - r) \left(\frac{g\pi}{N} - \frac{\pi f}{\Delta f} \right) \right)}{\sin \left((r + 1) \frac{\pi}{N} - \frac{\pi f}{\Delta f} \right)}$$

$$B_1 = \frac{\sin \left((N - r - 1) \left((L - g) \frac{\pi}{N} - \frac{L\pi f}{\Delta f} \right) \right)}{\sin \left((L - g) \frac{\pi}{N} - \frac{L\pi f}{\Delta f} \right)} \times$$

$$\times \frac{\sin \left(g \left((r + 1) \frac{\pi}{N} - \frac{\pi f}{\Delta f} \right) \right)}{\sin \left((r + 1) \frac{\pi}{N} - \frac{\pi f}{\Delta f} \right)}$$

$$k = rN + g; 0 \leq r \leq N-1; 0 \leq g \leq N-1$$

f – Doppler frequency shift.

Table 1

Complex matrix of the generalized Franck code

	0	1	.	L-2	L-1	L	.	M-1
0	$j0$ $1e$	$j0$ $1e$.	$j0$ $1e$	$j0$ $1e$	0	.	0
1	$j0$ $1e$	$j4\pi/N$ $1e$.	$j(L-2)2\pi/N$ $1e$	$j(L-1)2\pi/N$ $1e$	0	.	0
2	$j0$ $1e$	$54\pi/N$ $1e$.	$j(L-2)4\pi/N$ $1e$	$j(L-1)4\pi/N$ $1e$	0	.	0
.	0
N-1	$j0$ $1e$	$j(N-1)2\pi/N$ $1e$.	$j(L-2)(N-1)4\pi/N$ $1e$	$j(L-1)(N-1)4\pi/N$ $1e$	0	.	0

For $M \geq 2L$

$$\chi(\tau, f) = \begin{pmatrix} (A_2), \text{ for } 0 \leq g \leq L-1; \\ 0, \text{ for } L-1 < g < M-L+1; \\ (B_2), \text{ for } M-L+1 \leq g \leq M-1. \end{pmatrix} \quad (3)$$

where

$$A_2 = \frac{\sin\left((L-g)\left(\frac{r\pi}{N} - \frac{\pi f}{\Delta f}\right)\right) \sin\left((N-r)\left(\frac{g\pi}{N} - \frac{\pi f}{\Delta f}\right)\right)}{\sin\left(\frac{r\pi}{N} - \frac{\pi f}{\Delta f}\right) \sin\left(\frac{g\pi}{N} - \frac{M\pi f}{\Delta f}\right)} \quad (6)$$

$$B_2 = \frac{\sin\left((M-L-g)\left((r+1)\frac{\pi}{N} - \frac{\pi f}{\Delta f}\right)\right)}{\sin\left((r+1)\frac{\pi}{N} - \frac{\pi f}{\Delta f}\right)} \times \quad (7)$$

$$\times \frac{\sin\left((N-r-1)\left((M-g)\frac{\pi}{N} - \frac{M\pi f}{\Delta f}\right)\right)}{\sin\left((M-g)\frac{\pi}{N} - \frac{M\pi f}{\Delta f}\right)}$$

Because the given equations (2) and (3) are rather complex and hard for calculations by using computer, it was decided to form the signals as analytical signals, which have only the dependencies on an amplitude and phase multiplier, and the carrier frequency is supposed to be known.

The investigation of the complex polyphase signals was conducted by using a specially created computer program within MATLAB system. When $L=M=N$ the GFC transforms into a Franck code. By substituting $p=L/N=1$ into (2) and (3) we receive the equations for Frank code ambiguity function.

For $M=L$

$$\chi(\tau, f) = \sqrt{A_1^2 + B_1^2 + 2A_1B_1 \cos\left(\left(N^2 - 2N + 1\right)\frac{\pi}{N}\right)} \quad (4)$$

where

$$A_1 = \frac{\sin\left((N-g)\left(\frac{r\pi}{N} - \frac{\pi f}{\Delta f}\right)\right) \sin\left((N-r)\left(\frac{g\pi}{N} - \frac{\pi f}{\Delta f}\right)\right)}{\sin\left(\pi - \frac{g\pi}{N} - \frac{L\pi f}{\Delta f}\right) \sin\left((r+1)\frac{\pi}{N} - \frac{\pi f}{\Delta f}\right)}$$

$$B_1 = \frac{\sin\left((N-r-1)\left(\pi - \frac{g\pi}{N} - \frac{N\pi f}{\Delta f}\right)\right)}{\sin\left(\pi - \frac{g\pi}{N} - \frac{N\pi f}{\Delta f}\right)} \times$$

$$\times \frac{\sin\left(g\left((r+1)\frac{\pi}{N} - \frac{\pi f}{\Delta f}\right)\right)}{\sin\left((r+1)\frac{\pi}{N} - \frac{\pi f}{\Delta f}\right)}$$

$$k = rN + g; 0 \leq r \leq N-1, 0 \leq g \leq N-1$$

Below, the results of some characteristics of the GFC are given.

3. Results

For the GFC with the value of phase quantization $N=4$ and $p=1$ Fig.1 shows the autocorrelation function (ACF), the main lobe of which is rather wide and there is a significant level of side lobes. With the increase in the phase quantization value to 7 with $p=1$ the width of the main lobe of the ACF decreases and the level of the side lobes becomes lower (fig. 2).

The specter of the signal based on the GFC for $N=12$ and $p=0.5$, its ACF, frequency ACF and ambiguity function are shown on the fig. 3-6.

Analogically for the signal based on the GFC with $N=12$ and $p=1$ the corresponding characteristics are shown on the fig. 7-10, and on the fig. 11-14 for the signal based on the GFC with $N=12$ and $p=2$.

As the Figures show, the character of the specters of the signals based on the GFC for all N and p parameters is saved, but for $p < 1$ and $p > 1$ the specter will have the striped structure. The width of the stripes and their number in the lobes depends on the parameter p and phase quantization level N . Also the main lobe of the ACF is split, i.e. two side lobes with big amplitude appear.

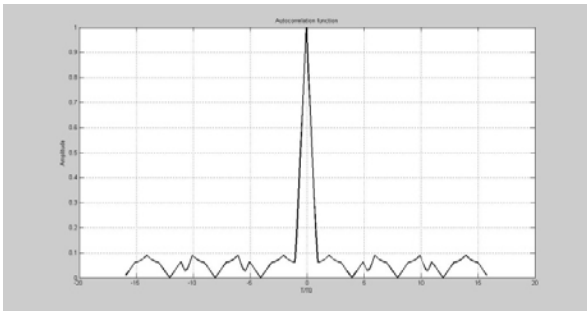


Fig. 1. Autocorrelation function of the signal based on the GFC with parameters $N=4$, $p=1$

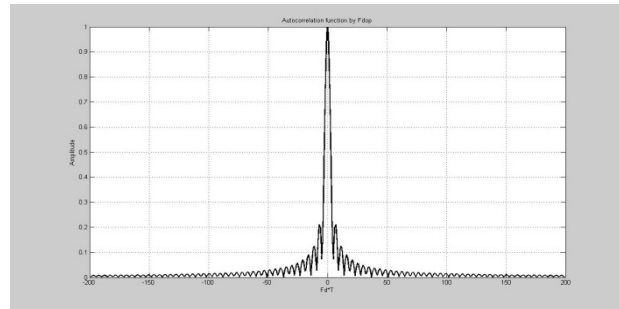


Fig. 5. Frequency-autocorrelation function of the signal based on the GFC with parameters $N=12$, $p=0.5$

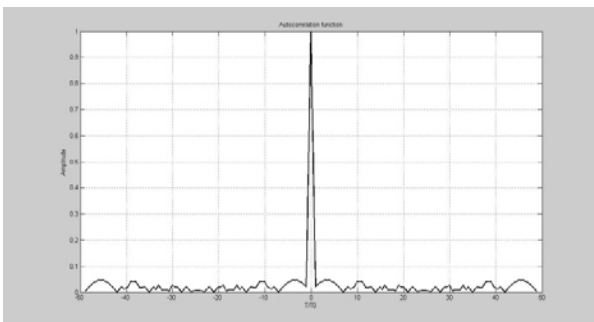


Fig. 2. Autocorrelation function of the signal based on the GFC with parameters $N=7$, $p=1$

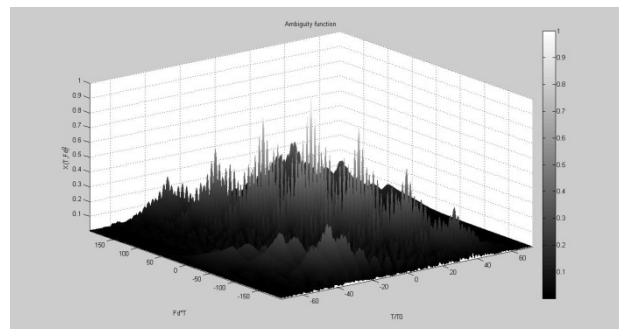


Fig. 6. Ambiguity diagram of the signal based on the GFC with parameters $N=12$, $p=0.5$

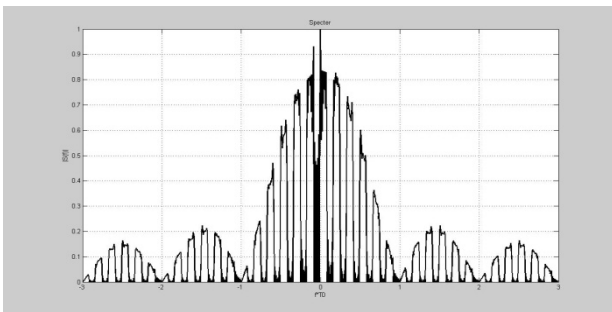


Fig. 3. . Specter of the signal based on the GFC with parameters $N=12$, $p=0.5$

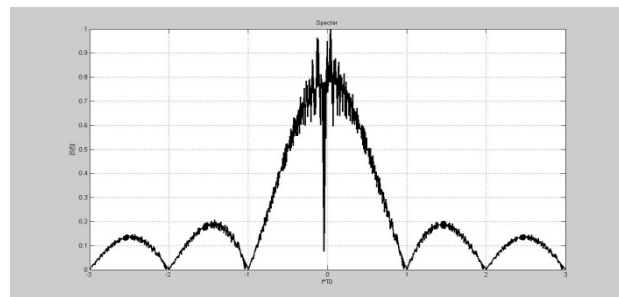


Fig. 7. Specter of the signal based on the GFC with parameters $N=12$, $p=1$

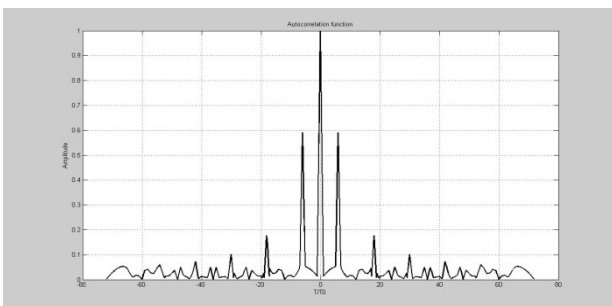


Fig. 4. Autocorrelation function of the signal based on the GFC with parameters $N=12$, $p=0.5$

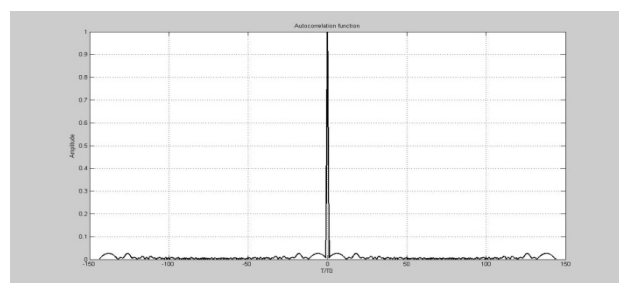


Fig. 8. Autocorrelation function of the signal based on the GFC with parameters $N=12$, $p=1$

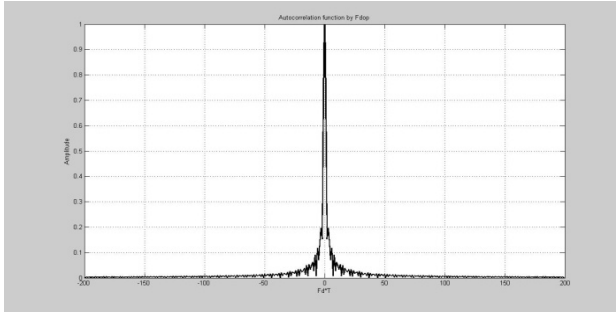


Fig. 9. Frequency-autocorrelation function of the signal based on the GFC with parameters $N=12$, $p=1$

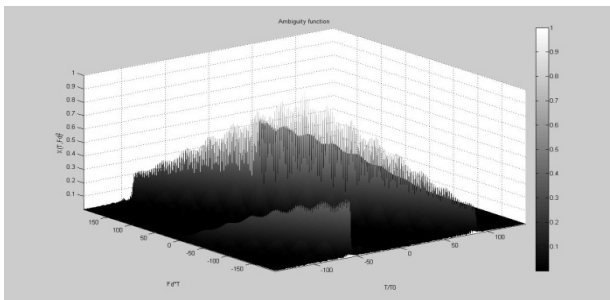


Fig. 10. Ambiguity function of the signal based on the GFC with parameters $N=12$, $p=1$

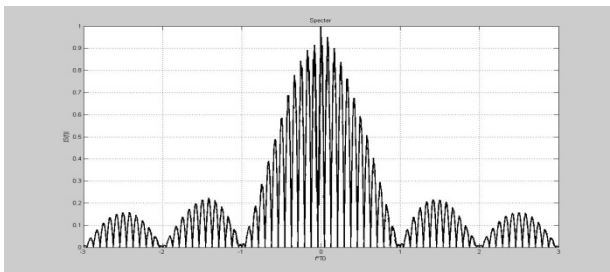


Fig. 11. Specter of the signal based on the GFC with parameters $N=12$, $p=2$

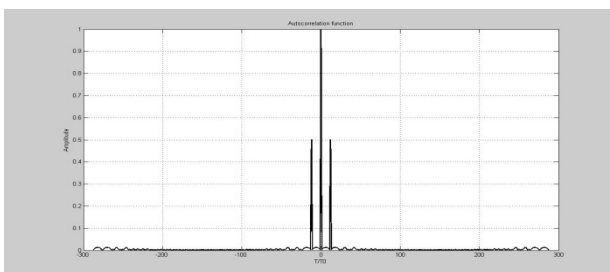


Fig. 12. Autocorrelation function of the signal based on the GFC with parameters $N=12$, $p=2$

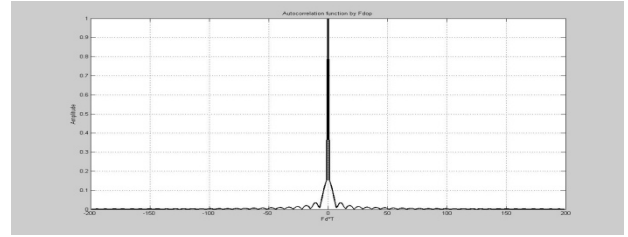


Fig. 13. Frequency-autocorrelation function of the signal based on the GFC with parameters $N=12$, $p=2$

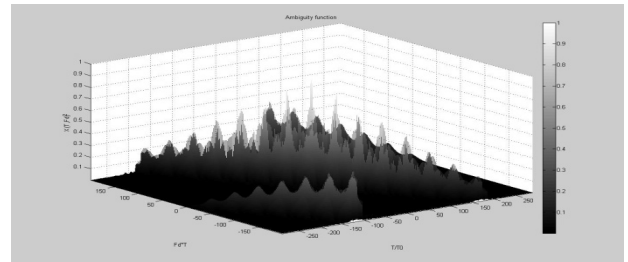


Fig. 14. Ambiguity function of the signal based on the GFC with parameters $N=12$, $p=2$

Besides, the ACF of the signal based on the GFC with $N=11$ and $p=1$ is shown in Fig. 15, and in Fig. 16 – for the signal with $N=16$ and $p=1$.

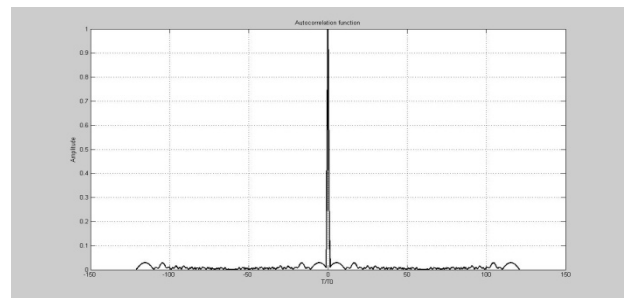


Fig. 15. Autocorrelation function of the signal based on the GFC with parameters $N=11$, $p=1$

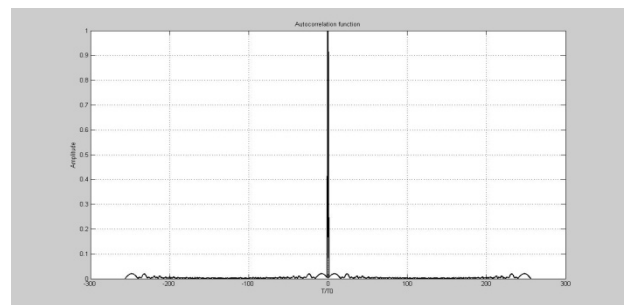


Fig. 16. Autocorrelation function of the signal based on the GFC with parameters $N=16$, $p=1$

For the signal with $p < I$ levels of the ambiguity pikes in the field $(fT) \leq N/2$ are defined by the equation

$$U' = \frac{2}{c\pi} \frac{\sin(\pi\eta(c + \eta/p))}{\sin(\pi\eta)}, c \leq N \quad (5)$$

where $\eta = \frac{fT}{N}$, c – ordinal number of the ambiguity spike.

For the signals with $p > 1$, the specter stripe's fronts are not so steep as the signals with $p < 1$ have. In these signal the main lobe of the ACF is split, i.e. two side lobes with a big amplitude appear. It is necessary to note that the specter striped structure and the split of the ACF main lobe does not have a great influence on the ambiguity diagram in general, as in the case of the signals based on the GFC with $p < 1$.

Levels of the ambiguity pikes in the field $(fT) \leq N/2$ are defined by the equation

$$U' = \left(\frac{\sin\left(\pi\eta\left(1 - \frac{c}{p} - \eta/p\right)\right)}{\pi\eta} \right), 0 \leq \eta \leq 1 \quad (6)$$

where $c = 1, 3, \dots$ – ordinal number of the ambiguity spike.

The important property of the signals based on the GFC is the side lobes decrease in the comparison with the signals, which are used in modern radars. So the numerical results of the side lobes levels for different signals are shown in Table 2, and their levels dependency on the phase quantization levels N for GFC is shown in Fig. 17. As we can see, with the growth of the N the level of the side lobes decreases.

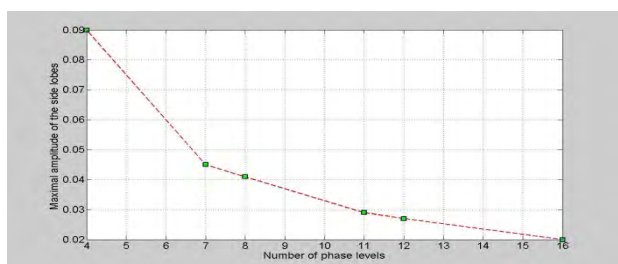


Fig. 17. Side lobes dependency of the signals based on the GFC with different parameters of N and $p=1$

Table 2

ACF side lobes levels for different types of the signals

Signal	Side lobe level, max
LFM	0,28
Barker code, 13-positional	0,1
Biphase recurrent code, 127-positional	0,07
5-pahse recurrent code, 124-positional	0,08 (0,05 mean)
Franck code, 11-pahse levels, 121-positional	0,029

4. Conclusions

The signals based on the GFC with the corresponding phase quantization levels give us an opportunity to form needle-shaped autocorrelation functions with low levels of the side lobes on the time-Doppler frequency field. Their use in the radar systems will lead to the growth of the system's resolution, hindrances immunity and reliability of the detection and recognition.

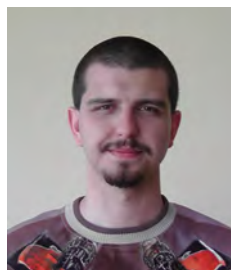
References

1. "Modern radar. Analysis, evaluation and system design", The Moore School of Electrical Engineering University of Pennsylvania, pp 204-216, 1965.
2. I. Prudyus, A. Zubkov, M. Sumyk, L. Lazko, D. Mymrikov, R. Yankevych "Postroyeniye mnogokanalnyh integrirovanyh system distancionnogo nabludeniya na base parcialnyh kanalov", CriMiCo 2010, Sebastopol, September 13-17, 2010.
3. M. Sumyk, I. Prudyus, R. Sumyk, "Teoriya sygnaliv", publication "Beskyd Bit", Lviv, 2008.
4. I. Prudyus, M. Sumyk, R. Yankevych "Investigation of phase coded signals based on generalized Frank codes", UWBUSIS 2010, Sebastopol, September 6-10, 2010.
5. P.A. Bakulev, "Radiolokacionnyye sistemy", publication «Radiotekhnika», Moscow, 2004.
6. Radar Systems Analysis and Design Using MATLAB. Bassem R. Mahafza, Ph.D. COLSA Corporation, Huntsville, Alabama.

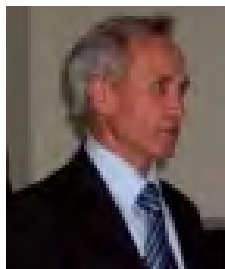
**ВЛАСТИВОСТІ
БАГАТОФАЗНИХ СИГНАЛІВ
НА БАЗІ УЗАГАЛЬНЕНИХ
КОДІВ ФРЕНКА**

Р. Янкевич, І. Прудиус, М. Сумик

Розглянуто результати дослідження багатофазних сигналів на базі узагальнених кодів Френка. Виведено залежності параметрів головних пелюстків функції невизначеності від кількості рівнів квантування фази. Також встановлено залежність рівня бокових пелюстків від кількості рівнів квантування фази.



Yankevych Roman, 2nd year post graduate, Department of Radio-Electronic Devices and Systems, Institute of Telecommunications, Radio-Electronics and Electronic Engineering. Basic directions of scientific research are theory of signals, signal processing, radar systems.



Prudyus Ivan, DSc, professor, director of the Institute of Tele-communications, Radio-Electronics and Electronic Engineering, Head of the Department of Radio-Electronic Devices and Systems. Basic directions of scientific research are antennas, antenna systems, multispectral monitoring systems and complexes.



Markiyan Sumyk, PhD, professor of the Department of Radio-Electronic Devices and Systems, Institute of Tele-communications, Radio-Electronics and Electronic Engineering. Basic directions of scientific research are theory of signals, signal processing, radar systems.